UDC 530.182

CONTROL OF BISTABILITY, OSCILLATIONS AND CHAOS IN A MODEL ELECTROCATALYTIC PROCESS ON A SPHERICAL ELECTRODE SURFACE

O.I. Gichan

Chuiko Institute of Surface Chemistry of National Academy of Sciences of Ukraine
17 General Naumov Street, Kyiv 03164, Ukraine

The role of a preceding chemical reaction in the appearance of three dynamical instabilities leading to multistability of steady states, periodic current oscillations, and possible chaotic behavior in a model electrocatalytic process on a spherical electrode surface under potentiostatic conditions has been determined. A class of non-equilibrium systems where these instabilities can arise was sketched out and possible applications of these instabilities were presented from recent literature data. The results obtained are actual and fruitful in context of nonlinear dynamics and can help to understand the processes at interfaces.

INTRODUCTION

The first observation of spontaneous periodic oscillations during an electrochemical surface reaction is dated back to 1828. As earlier as 1900 electrochemical oscillations indicated chaos was reported, but at that time this term had not yet been used. Since then the experimental evidence of electrochemical instabilities leading to various types of nonlinear behavior including multistability, periodicity, quasiperiodicity, and chaos have been constantly accumulating [1, 2]. The mentioned nonlinear effects can be undesirable, but in some cases they can be exploited as to obtain new functional materials, including nanostructured ones [3], to increase reaction rates and yields [4–12], to devise an electrode with certain properties [13, 14]. The experimental and theoretical interest to these questions has also been renewed with the appearance of a new paradigm in chaos theory – the possibility to control chaotic behavior of a non-equilibrium system by application of small perturbations to it [15]. Today there is an attempt to use the patterns of chaos to encode and to manipulate inputs so as to produce a desired output. The resultant morphing logic gates are termed chaogates [16]. Chaos, including well-defined transitions to chaos, has been observed numerous times in electrochemistry [17–28]. As the dynamical instabilities in electrochemical systems can be monitored by simple current or voltage measurements and parametric changes can be easily achieved by current or voltage control, electrochemical systems seem to be an ideal playground for testing different control strategies. This not only helps to unravel the origin of instabilities in electrochemical systems but also can help to shed light on mechanisms of such self-organization phenomena in other non-equilibrium systems, including those of practical relevance [29–31].

In the paper, the method of impedance spectroscopy is applied to quantitatively characterize three dynamical instabilities, namely, a Hopf instability, a saddle-node instability, and a homoclinic instability in a model electrocatalytic process on a spherical electrode which is preceded by a homogeneous chemical reaction in bulk solution under potentiostatic control.

THEORETICAL PART

The model process can be schematically written as

$$B_{bulk} \underset{k_2}{\overset{k_1}{\rightleftarrows}} A_{bulk} \rightarrow A_{surf} \underset{k_d}{\overset{k_a}{\rightleftarrows}} A_{ads} \xrightarrow{K_e} P + e, \quad (1)$$

where k_1, k_2 are the rate constants of chemical reaction in the bulk solution, and k_a, k_d, K_e are the rate constants of adsorption, desorption, and electron transfer, respectively. The last step of the reaction is considered to be irreversible.

This model electrocatalytic reaction was proposed for a theoretical explanation of spontaneous current/potential oscillations during electrooxidation of small organic molecules such as those of formaldehyde, methanol, ethanol, ethylene glycol, etc. on Pt electrode and other noble ones. These molecules were tested for their pos-

* corresponding author *gichan@isc.gov.ua*

sible application in fuel cells [32–34]. We added into the stage of a preceding chemical reaction in a near-electrode layer the reaction scheme [35–39]. Our interest was motivated by similar studies on influence of a preceding chemical reaction on impedance spectra [40].

Neglecting the Ohmic losses and double layer influence, we can write the rates of adsorption-desorption and electron transfer as follows:

$$\nu_1(\theta(t), c(r_0,t)) = \Gamma k_a \exp(\gamma\theta(t)/2)\, c(r_0,t) \times \times(1-\theta(t)) - \Gamma k_d \exp(-\gamma\theta(t)/2)\,\theta(t), \quad (2)$$

$$\nu_2(t) = \Gamma K_e(t)\theta(t) = \Gamma k_{\ e} \exp(\alpha b E(t))\theta(t). \quad (3)$$

Here, $c(r_0,t)$ is the concentration of electroactive species at the electrode surface, r_0 is the radius of the spherical electrode, $\theta(t)$ is the coverage of the electrode surface with the adsorbate, γ is the attraction constant, Γ is the maximum surface concentration at $\theta(t)=1$, F is the Faraday's number, R is the gas constant, T is the absolute temperature, α is the symmetry factor of electron transfer in the direction of oxidation, E is the electrode potential, $b = F/RT$, k_e is the rate constant of electron transfer at $E(t)=0$.

According to Eq. (2) the adsorption-desorption of species A on the electrode surface under steady-state conditions is described by the Frumkin isotherm [41]. Positive values of the attraction constant γ correspond to the attraction between adsorbed species, and its negative values correspond to the repulsion between adsorbed species. Only positive value of the attraction constant leads to instability [32–34]. In general, γ depends on potential [42, 43]. The adsorption equilibrium constant k_a/k_d can also be a function of the potential. We considered a case when γ is a constant and the adsorption-desorption rate constants are independent on the potential. As the control parameters we take γ and the effective rate of a preceding homogeneous chemical reaction k.

The changes in the electrode surface coverage θ with adsorbate and in the concentration $c(r, t) = c_0 + u$ (u is a deviation of concentration from equilibrium concentration c_0 corresponding to bulk concentration) satisfy the following equations:

$$\Gamma \frac{d\theta}{dt} = \nu_1(t) - \nu_2(t), \quad (4)$$

$$\frac{\partial c(r,t)}{\partial t} = D\frac{1}{r^2}\frac{\partial}{\partial r}\left(r^2 \frac{\partial c(r,t)}{\partial r}\right) - kc \quad (5)$$

with boundary conditions

$$J_c(r_0,t) = -D\frac{\partial c(r,t)}{\partial r}\Big|_{r=r_0} = -\nu_1(t),$$
$$c(\delta,t) = c_0,\ \delta = r_0 + d, \quad (6)$$

where k is the effective rate of a preceding homogeneous chemical reaction, D is the diffusion coefficient, d is the Nernst diffusion layer thickness. The origin of coordinates coincides with the center of the spherical electrode.

The faradaic current density is determined by the following equation:

$$i_f(t) = F\nu_2(t) = F\Gamma k_e \exp[\alpha b E(t)]\theta(t). \quad (7)$$

Steady-State Condition. The solution of the diffusion equation (5, 6) under steady-state conditions yields the following expressions for the steady-state electrode potential E_{st}, the steady-state concentration at the electrode surface $c_{st}(r = r_0)$ and the steady-state faradaic current density i_{fst}

$$E_{st} = (\alpha b)^{-1} \ln\left[\frac{m_c^*(c_0 - c_{st}(r_0))}{\Gamma k_e \theta_{st}}\right], \quad (8)$$

$$c_{st}(r_0) = \frac{m_c^* c_0 + \Gamma k_d \theta_{st} e^{-\gamma\theta_{st}/2}}{m_c^* + (1-\theta_{st})\Gamma k_a e^{\gamma\theta_{st}/2}}, \quad (9)$$

$$i_{fst} = F m_c^*(c_0 - c_{st}(r_0)), \quad (10)$$

where $m_c^* = m_c \dfrac{1+\varepsilon G_0}{G_0}$, $m_c = \dfrac{D}{d}$, $\varepsilon = \dfrac{d}{r_0}$, $G_0 = \dfrac{th\sqrt{\tau_d k}}{\sqrt{\tau_d k}}$, $\tau_d = \dfrac{d^2}{D}$ (τ_d is diffusion time of relaxation).

As in the calculations we neglected the electrolyte resistance and did not take into account the double layer impedance, that of the model system is equal to the faradaic one.

Hopf bifurcation and impedance spectra. It is known that the origin of electrochemical instabilities stems from the negative impedance characteristics of the faradaic processes at the electrode surface [32–34]. For potentiostatic conditions the study of the linear stability of an electrochemical system near its steady state is based on the analysis of the system impedance zeroes with changes of electrode potential [44]. The sign of the real part of impedance zero indicates the stability region of the stationary state [45]. As was

shown, a Hopf bifurcation can realize when complex impedance of electrochemical system is equal to zero at nonzero frequency, $Z(\omega)=0$ at $\omega=\omega_H\neq 0$ ($\omega=2\pi f$, f – frequency) [32–39, 44–49]. At Hopf bifurcation the system produces its own undammed periodic oscillations with frequency ω_H, so in the case of influence on the system of an external signal with a frequency exactly coinciding with this value, the external signal will pass through the system without resistance. In many cases a Hopf bifurcation is a prerequisite for more complex dynamical behavior, including chaos.

To calculate the faradaic impedance of this system, we consider its dynamic behavior when a low periodical signal is applied to the steady-state polarization potential

$$E(t)=E_{st}+\Delta E_0 e^{j\omega t}, \qquad (11)$$

where $j=\sqrt{-1}$, ω – angular frequency ($\omega=2\pi f$, f – frequency), ΔE_0 – amplitude of small periodic signal.

In response to this excitation the electrode surface coverage $\theta(t)$ oscillates near steady-state value as the faradaic current $i_f(t)$ and concentration $c(r_0, t)$ do.

$$\theta(t)=\theta_{st}+\Delta\theta_0 e^{j\omega t},\ i_f(t)=i_{fst}+\Delta i_f(E,\theta)$$
$$c(r_0,t)=c_{st}(r_0)+\Delta c(r_0,\theta). \qquad (12)$$

The faradaic impedance in the Laplace image space $\bar{F}(s)=\int_0^\infty f(t)e^{-st}dt$ is expressed as a function of complex frequency:

$$\bar{Z}(s)=\frac{\Delta\bar{E}(s)}{\Delta\bar{i}_f(s)}. \qquad (13)$$

Omitting some mathematical computations, the resultant expression for the faradaic impedance in the Laplace space can be written as:

$$\bar{Z}_f(s)= = R_{ct}\{1+\frac{\partial_\theta\nu_2[1+\varepsilon G(1+\mu\partial_c\nu_1)]}{\Gamma s[1+\varepsilon G(1+\mu\partial_c\nu_1)]-\partial_\theta\nu_1(1+\varepsilon G)}\}, \qquad (14)$$

where

$$R_{ct}=\frac{1}{\dfrac{\partial i_{fst}}{\partial E_{st}}}=\frac{1}{F\Gamma\alpha fk_e\exp(\alpha fE_{st})\theta_{st}} \qquad (15)$$

(charge transfer resistance),

$$G=\frac{th\sqrt{\tau_d(k+s)}}{\sqrt{\tau_d(k+s)}} \qquad (16)$$

(finite length Gerischer impedance),

$$\partial_\theta\nu_1=\Gamma\{k_d\exp(-\gamma\theta_{st}/2)[\gamma\theta_{st}/2-1]+ +k_a\exp(\gamma\theta_{st}/2)c_{st}(r_0)[\gamma(1-\theta_{st})/2-1]\}, \qquad (17)$$

$$\partial_c\nu_1=\Gamma k_a(1-\theta_{st})\exp(\gamma\theta_{st}/2), \qquad (18)$$

$$\partial_\theta\nu_2=\Gamma k_e\exp(\alpha bE_{st}), \qquad (19)$$

$$\mu=r_0/D. \qquad (20)$$

For sake of convenience, the partial derivatives are designated here as $\partial_x u=\partial u/\partial x$.

Thus, to find the Hopf bifurcation points of the system, the zeros of impedance $\bar{Z}_f(s)$ depending on electrode potential must be studied. In our case, the impedance zeros can be found from the following equation:

$$\Psi(k,s,\theta)=(\Gamma s+\partial_\theta\nu_2)[1+\varepsilon G(1+\mu\partial_c\nu_1)]- -\partial_\theta\nu_1(1+\varepsilon G)=0. \qquad (21)$$

This is the equality to zero of the numerator of Eq. (14).

To satisfy the condition (22), it is necessary that

$$\begin{cases}\mathrm{Re}[\Psi(s,\theta,k)]=0\\ \mathrm{Im}[\Psi(s,\theta,k)]=0.\end{cases} \qquad (22)$$

Eq. (22) can be solved only numerically. The intersection of the obtained surfaces gives the Hopf bifurcation points, namely, bifurcation values of frequency ω_H, electrode surface coverage by adsorbate θ_H and the effective rate of a preceding chemical reaction k_H. In order to pass from the Laplace space to the Fourier space, it is necessary to perform a substitution $s=j\omega$.

Saddle-node bifurcation and polarization resistance. The saddle–node bifurcation indicates the realization in a non-equilibrium system bistability – the coexistence of two stable steady states at the same values of the parameters [32–34, 36, 49]. The bistability region is that where the system can be in one of two stable steady state. Which one is chosen depends on where the system comes from, i.e. on initial conditions. In this sense the bistable system has a memory. The saddle-node bifurcations always come in pairs and lead to hysteresis.

The saddle–node bifurcation points can be found from equality to zero of an electrochemical system polarization resistance. As well known, polarization resistance is equal to the system impedance at $\omega\to 0$, $Z_P=\lim_{\omega\to 0}Z_f(\omega)$.

In our case the system polarization resistance has the form

$$Z_P=R_{ct}\{1+\frac{\partial_\theta\nu_2[1+\varepsilon G_0(1+\mu\partial_c\nu_1)]}{-\partial_\theta\nu_1(1+\varepsilon G_0)}\}, \qquad (23)$$

To find bifurcation values of electrode surface coverage by adsorbate θ_{SN1} and θ_{SN2} that confine the bistability region, we should solve Eq. 24

$$Z_P = 0. \qquad (24)$$

This can be done only numerically.

Homoclinic bifurcation – complex dynamics. Since Poincaré's pioneering work, orbits which are homoclinic to saddle periodic ones have been one of the most attractive objects under study in the theory of dynamical systems. The main reason to study homoclinic orbits is that their presence implies complicated dynamics, including chaotic one [20, 34, 50–52]. A homoclinic bifurcation occurs if an oscillatory state collides with a stationary state of the saddle type (in phase plane of dynamical variables at critical parameter value the limit cycle – oscillatory solution of the system born in a Hopf bifurcation, connects to the saddle in a homoclinic orbit). The homoclinic orbit is an oscillatory state of infinite period. When approaching a critical parameter value, the period of the oscillations will grow logarithmically, beyond the bifurcation, oscillations no longer occur.

In our case a homoclinic bifurcation is realized in the system when the bifurcation values of the electrode surface coverage by adsorbate θ_{SN1} and θ_H approach each other.

In the model calculations, the following values of the system parameters were taken: $\Gamma = 10^{-9}$ mol·cm^{-2}; $\gamma = \{5; 8\}$; $\Gamma k_a = 0.1$ cm·s^{-1}; $\Gamma k_d = 10^{-5}$ mol/cm^2·s; $k_e = 10$ s^{-1}; $D = 10^{-5}$ cm^2/s; $d = 10^{-3}$ cm; $\alpha = 0.5$; $c_0 = 10^{-5}$ mol/cm^3; $F = 96484$ C/mol; $R = 8{,}314$ J/mol·K; $T = 300$ K; $b = 38{,}7$ V^{-1}, $r_0 = 10^{-2}$ cm.

All numerical calculations were performed with the mathematical package Mathematica™ [53].

RESULTS AND DISCUSSION

We have an electrochemical system of the N-NDR type [2]. In this system the electrode potential plays the role of an activator and the concentration of electroactive species in the near-electrode layer plays the role of an inhibitor.

We considered changes in the system dynamics at two values of the attraction constant, namely, $\gamma = 8$ and $\gamma = 5$. In both cases the steady-state polarization curves i_{fst} vs. E_{st} of the model process have a region of the potentials with the negative slope, where $di_f / dE < 0$. This is so-called negative differential resistance (NDR) region where a Hopf instability usually occurs. In the second case the distorted steady-state polarization curves have also a region of bistability, where two values of the faradaic current density corresponds to one value of the electrode potential. In both cases an increase in the preceding chemical reaction rate, k, leads to an increase in the faradaic current density as for a plane electrode [35–39].

Fig. 1 shows the surfaces of zeros of the functions $\mathrm{Re}[\Psi(s,\theta,k)]$ and $\mathrm{Im}[\Psi(s,\theta,k)]$ for the chosen values of the attraction constant γ. The line of their intersection is the solution of Eq. (22) – the Hopf bifurcation points of the system.

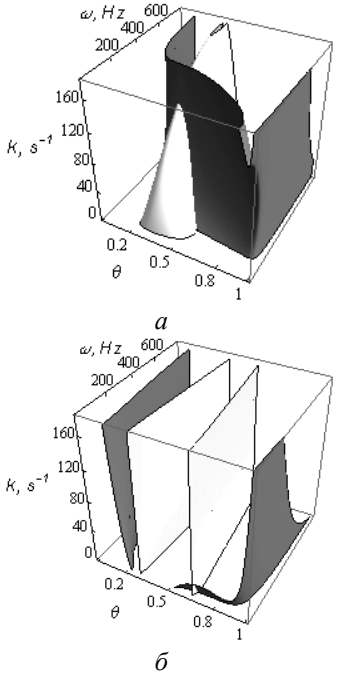

Fig. 1. Surfaces of zeros of the system impedance real (light) and imaginary (dark) parts: $a - \gamma = 8$, $b - \gamma = 5$

As it is seen from Fig. 1, in case of the higher value of the attraction constant we can always find two Hopf bifurcation points at a fixed value of the parameter k, up to its threshold value k_{th}. For the values of k higher than this threshold value k_{th} ($k_{th} \approx 132$ s^{-1}) the system remains stable to the Hopf bifurcation, and periodic oscillations are absent. For $\gamma = 5$ the threshold value k_{th} ($k_{th} \approx 16$ s^{-1}) is lower and the system has only one Hopf bifurcation point up to this value of preceding chemical reaction rate. An increase of k shifts the bifurcation frequency ω_H to the region of lower values in contrast to the case of $\gamma = 8$.

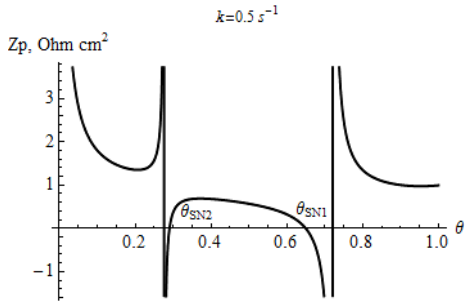

Fig. 2. The system polarization resistance Z_p vs. θ at a given value of the parameter k

Figure 2 presents dependence of the system polarization resistance Z_P on the value of θ at a given value of the parameter k. Intersection of the $Z_P(\theta)$ curve with the abscess axis yields two bifurcation values of the electrode surface coverage by adsorbate at which a saddle – node bifurcation appears in the system (the system impedance turns to zero at the zero frequency). A change in parameter k effects practically no changes in the bifurcation values θ_{SN} (see Tables 1 and 2). At $\gamma = 8$ the saddle– node bifurcation is not realized in the system – the $Z_P(\theta)$ curve does not cross the abscess axis, as the shape of the voltammetric curve changes, i.e. there is no bistability.

Table 1. The electrochemical system parameters in the Hopf and the saddle–node bifurcation points at $k = 0.5$ s^{-1} and $\gamma = 5$

Points of bifurcation	ω, Hz	θ	i_{fst}, A cm^{-2}	E_{st}, V
Hopf	28.72	0.6632	0.002891	0.077930
saddle-node	0	0.6496	0.002836	0.078008
saddle-node	0	0.2904	0.000420	0.020918

Table 2. The electrochemical system parameters in the Hopf and the saddle–node bifurcation points at $k = 15$ s^{-1} and $\gamma = 5$

Points of bifurcation	ω, Hz	θ	i_{fst}, A cm^{-2}	E_{st}, V
Hopf	10.61	0.6505	0.003868	0.093974
saddle-node	0	0.6491	0.003860	0.093974
saddle-node	0	0.2903	0.000569	0.036654

Tables 1 and 2 indicate that the bifurcation values of electrochemical parameters in the Hopf bifurcation point and one of the saddle–node bifurcation points are very close. Such a feature of the system is retained in the whole range of values of the parameter $k < k_{th}$. This is the case of positive implementation of a homoclinic bifurcation into the system as for a plane electrode [36].

CONCLUSION

On the basis of the theory of electrochemical impedance spectroscopy the necessary conditions for the appearance of three dynamical instabilities causing multistability of steady-states, periodic and chaotic oscillations has been obtained in a model electrocatalytic process on a spherical electrode surface under potentiostatic conditions.

It was shown that the emergence of some of these dynamical instabilities may be regulated by the rate of the preceding homogeneous chemical reaction in the bulk solution. The spontaneous periodic oscillations can arise in the system at the rates of this reaction which are lower than some threshold value, k_{th}, whereas at higher values of this parameter the system does not undergo such an instability.

The appearance of bistability in the system is determined by the value of the attraction constant, γ, in the Frumkin isotherm and is less dependent on the values of parameter k. At $\gamma = 8$ we can observe only spontaneous periodic oscillations, while at $\gamma = 5$, both oscillations and bistable states are possible in the system and even more complex dynamical behavior evoked by realization of a homoclinic bifurcation.

REFERENCES

1. *Hudson J.L., Tsotsis T.T.* Electrochemical Reaction Dynamics. Review // Chem. Eng. Sci. – 1994. – V. 49. – P. 1493–1572.
2. *Krischer K.* Spontaneous formation of spatiotemporal patterns at the electrode | electrolyte interface. Review // J. Electroanal. Chem. – 2001. – V. 501. – P. 1–21.
3. *Eskhult J., Ulrich C., Björefors F., Nyholm L.* Current oscillation during chronoamperometric and cyclic voltammetric measurements in alkaline Cu(II)-citrate solutions // Electrochim. Acta. – 2008. – V. 53. – P. 2188–2197.
4. *Chen S., Lee D., Schell M.* Enhancement of the electrochemical oxidation of formic acid. Effects of anion adsorption and variation of rotation rate // Electrochim. Acta. – 2001. – V. 46. – P. 3481–3492.
5. *Punckt C., Stich M., Beta C., Rotermund H.* Suppression of spatiotemporal chaos in the oscillatory CO oxidation on Pt(110) by focused laser light // Phys. Rev. E. – 2008. – V. 77. – P. 046222–046234.
6. *Morschl R., Bolten J., Bonnefont A., Krischer K.* Pattern formation during CO electrooxidation on Thin Pt films studied with spatially resolved infrared absorption spectroscopy // J. Phys. Chem. C. – 2008. – V. 112. – P. 9548–9551.
7. *Malkhandi S., Bonnefont A., Krischer K.* Dynamic instabilities during the continuous electro-oxidation of CO on poly- and single crystalline Pt electrodes // Surf. Sci. – 2009. – V. 603, N 10–12. – P. 1646–1651.

8. *Christoph J., Noh T.-G., Lee J. et al.* Spatiotemporal self-organization in the oscillatory HCOOH oxidation on a Pt ribbon electrode – Theory and experiments // Surf. Sci. – 2009. – V. 603, N 10–12. – P. 1652–1661.
9. *Kiss I.Z., Munjal N., Martin R.S.* Synchronized current oscillations of formic acid electro-oxidation in a microchip-based dual-electrode flow cell // Electrochim. Acta. – 2009. – V. 55. – P. 395–403.
10. *Swamy B.E.K., Vannoy C., Maye J. et al.* Potential oscillations in formic acid oxidation in electrolyte mixtures: Efficiency and stability // J. Electroanal. Chem. – 2009. – V. 625. – P. 69–74.
11. *Mota A., Lopes P.P., Ticianelli E.A. et al.* Complex oscillatory response of a PEM fuel cell fed with H_2/CO and oxygen // J. Electrochem. Soc. – 2010. – V. 157, N 9. – P. B1301–B1304.
12. *Garcia-Morales V., Krischer K.* Fluctuation enhanced electrochemical reaction rates at the nanoscale // PNAS. – 2010. – V. 107, N 10. – P. 4528–4532.
13. *Mazouz N., Krischer K.* A theoretical study on Turing patterns in electrochemical systems // J. Phys. Chem. B. – 2000. – V. 104, N 25. – P. 6081–6090.
14. *Li Y.J., Oslonovitch J., Mazouz N. et al*. Turing-type patterns on electrode surfaces // Science. – 2001. – V. 291. – P 2395–2398.
15. *Shinbrot T., Grebogi C., Ott E., Yorke J.A.* Using small perturbations to chaos. Review // Nature. – 1993. – V. 363. – P. 411–417.
16. *Ditto W.L, Miliotis A., Murali K. et al.* Chaogates: Morphing logic gates that exploit dynamical patterns // Chaos. – 2010. – V. 20. – P. 037107–037114.
17. *Eiswirth M., Krischer K., Ertl G.* Transition to chaos in an oscillating surface reaction // Surf. Sci. – 1988. – V. 202, N 3. – P. 565–591.
18. *Bassett M.R., Hudson J.L.* Experimental evidence of period doubling of tori during an electrochemical reaction // Physica D. – 1989. – V. 35, N 3. – P. 289–298.
19. *Albahadily F.N., Schell M.* Observation of several different temporal patterns in the oxidation of formic acid at a rotating platinum-disk electrode in an acidic medium // J. Electroanal. Chem. Interfacial Electrochem. – 1991. – V. 308, N 1–2. – P. 151–173.
20. *Argoul F., Huth J., Merzeau P. et al.* Experimental evidence for homoclinic chaos in an electrochemical growth process // Physica D. – 1993. – V. 62, N 1–4. – P. 170–185.
21. *Green B.J., Wang W., Hudson J.L.* Chaos and spatiotemporal pattern formation in electrochemical reactions. Review // Forma. – 2000. – V. 15. – P. 257–265.
22. *Parkhutik V.* Chaos-order transitions at corroding silicon surface // Mater. Sci. Eng. B. – 2002. – V. 88. – P. 269–276.
23. *Siegmeier J., Baba N., Krischer K.* Bistability and oscillations during electrooxidation of H_2-CO mixtures on Pt: Modeling and bifurcation analysis // J. Phys. Chem. C. – 2007. – V. 111. – P. 13481–13489.
24. *Birzu A., Krischer K.* Confined Spatio-temporal chaos during metal electrodissolution: simulations // Zeitschrift fur Physikalische Chemie. – 2007. – V. 221. – P. 1245–1254.
25. *Baba N., Krischer K.* Mixed-mode oscillations and cluster patterns in an electrochemical relaxation oscillator under galvanostatic control // Chaos. – 2008. – V. 18. – P. (015103) 1–4.
26. *Noh T.* Shil'nikov chaos in the oxidation of formic acid with bismuth ion on Pt ring electrode // Electrochim. Acta. – 2009. – V. 54. – P. 3657–3661.
27. *Lashina E.A., Chumakova N.A, Chumakov G.A., Boronin A.I.* Chaotic dynamics in the three-variable kinetic model of CO oxidation on platinum group metals // Chem. Eng. J. – 2010. – V. 154, N 1–3. – P. 82–87.
28. *Massoudi A., Mahjani M.G., Jafarian M.* Multiple attractors in Koper–Gaspard model of electrochemical periodic and chaotic oscillations // J. Electroanal. Chem. – 2010. – V. 647, N 1. – P. 74–86.
29. *Sadeghi S., Thompson M*. Towards information processing from nonlinear physical chemistry: A synthetic electrochemical cognitive system // Biosystems. – 2010. – V. 102, N 2–3. – P. 99–111.
30. *Moskalenko O.I., Koronovskii A.A., Hramov A.E.* Generalized synchronization of chaos for secure communication: Remarkable stability to noise // Phys. Lett. A. – 2010. – V. 374, N 29. – P. 2925–2931.
31. *Purwins H.-G., Bodeker H.U., Amiranashvili S.* Dissipative solitons // Adv. Phys. – 2010. – V. 59, N 5. – P. 485–701
32. *Koper M.T.M., Sluyters J.H.* Instabilities and oscillations in simple models of electrocatalytic surface reactions // J. Electroanal. Chem. – 1994. – V. 371. – P. 149–159.
33. *Koper M.T.M.* Stability study and categorization of electrochemical oscillations by impedance spectroscopy // J. Electroanal. Chem. – 1996. – V. 409. – P. 175–182.
34. *Koper M.T.M.* Non-linear phenomena in electrochemical systems // J. Chem. Soc. Faraday Trans. – 1998. – V. 94, N 10. – P. 1369–1378.
35. *Pototskaya V.V., Gichan O.I., Omelchuk A.A.* Influence of kinetic parameters of a preceding chemical reaction on appearance of instability in an electrochemical system with electrocatalytic oxidation // Dopovidi NANU. – 2011. – N 2. – P. 130–136 (in Russian).
36. *Pototskaya V.V., Gichan O.I.* Dynamic instabilities of a model electrochemical system with electrochemical oxidation and preceding chemical reaction // Rus. J. Electrochem. – 2011. – V. 47. – P. 336–344.
37. *Pototskaya V.V., Gichan O.I., Omel'chuk A.A.* Predicting the onset of spontaneous oscillations using impedance method // JCAAM. – 2011. – V. 9, N 1. – P. 68–75.
38. *Pototskaya V.V., Gichan O.I., Omel'chuk A.A.* Effect of preceding chemical reaction rate on dynamical instability in an electrochemical system // Oscillations and Pattern Formation in Electrochemistry: Proc. 218th Electrochemical Society Meeting (10–15 Oct. 2010, Las Vegas, USA). – Abstr. 2238.
39. *Pototskaya V.V., Gichan O.I., Omel'chuk A.A.* Impedance analysis of model electrocatalytic process with Frumkin adsorption isotherm occurring on spherical and flat elec-

trodes // Electrochemical Technologies and Materials for XXI Century: Proc. 9th International Frumkin Symposium (24–29 Oct. 2010, Moscow). – P. 45.
40. *Gerischer H.* Wechselstrom Polarisation von Elektroden mit einem Potentialbestimmenden Schritt beim Gleichgewichtspotential // Zeitschrift fur Physikalische Chemie. – 1951. – Bd. 198. – S. 286–314.
41. *Frumkin A.N.* Die Kapillarkurve der hoheren Fettsauren und die Zustandsgleichung der Oberflachenschicht // Zeitschrift fur Physikalische Chemie. – 1925. – Bd. 116. – S. 466–473.
42. *Damaskin B.B., Safonov V.A., Baturina O.A.* Statistical method of determining adsorption parameters for simple organic compounds from nonequilibrium differential capacitance // Rus. J. Electrochem. – 1997. – V. 33. – P. 105–115.
43. *Damaskin B.B., Safov V.A.* Regression analysis of electrocapillary curves in ethylforate solutions // Rus. J. Electrochem. – 2005. – V. 41. – P. 253–262.
44. *Naito M., Tanaka N., Okamoto H.* General relation between complex impedance and linear stability in electrochemical systems // J. Chem. Phys. – 1999. – V. 111. – P. 9908–9917.
45. *Berthier F., Diard J.-P, Montella C.* Hopf bifurcation and sign of the transfer resistance // Electrochim. Acta. – 1999. – V. 44. – P. 2397–2404.
46. *Pototskaya V.V., Gichan O.I., Omel'chuk A.A., Volkov S.V.* Specific features of the behavior of an electrochemical system in the case of the Hopf instability for a spherical electrode // Rus. J. Electrochem. – 2008. – V. 44. – P. 594–601.
47. *Pototskaya V.V., Gichan O.I., Omel'chuk A.A.* Electrode geometry and Hopf instability // Rus. J. Electrochem. – 2010. – V. 46. – P. 494–500.
48. *Pototskaya V.V., Gichan O.I., Omel'chuk A.A.* Unstable states at interfaces of spherical geometry // Ukr. Fiz. Zh. – 2010. – V. 55, N 7. – P. 836–840.
49. *Berthier F., Diard J.-P., Nugues S.* On the nature of the spontaneous oscillations observed for the Koper-Sluyters electrocatalytic reaction // J. Electroanal. Chem. – 1997. – V. 436. – P. 35–42.
50. *Gavrilov N.K., Shilnikov L.P.* Three-dimensional dynamical systems close to systems with a structurally unstable homoclinic curve // Mathematics of the USSR-Sbornik. – 1973. – V. 19. – P. 139–156.
51. *Turaev D.* On dimension of non-local bifurcational problems // Int. J. Bifurcation and Chaos. – 1996. – V. 6. – P. 123–156.
52. *McCullen N.J., Moresco P.* Route to hyperchaos in a system of coupled oscillators with multistability // Phys. Rev. E. – 2011. – V. 83. – P. (046212)1–9.
53. *Wolfram S.* Mathematic: a System for Doing Mathematics by Computer. – Redwood City: Addison Wesley, 1988. – 749 p.

Received 26.05.2011, accepted 06.06.2011

Контроль бістабільності, осциляцій та хаосу в модельному електрокаталітичному процесі на поверхні сферичного електроду

О.І. Гічан

Інститут хімії поверхні ім. О.О. Чуйка Національної академії наук України
вул. Генерала Наумова 17, Київ 03164, Україна, gichan@isc.gov.ua

Визначена роль попередньої хімічної реакції у появі трьох динамічних нестійкостей, що ведуть до мультистабільності стаціонарних станів, періодичних осциляцій струму і можливої хаотичної поведінки в модельному електрокаталітичному процесі на поверхні сферичного електрода за потенціостатичних умов. Представлено стислий огляд класу нерівноважних систем, де виникають такі нестійкості, та розглянуто їхнє можливе застосування за останніми літературними даними. Отримані результати є актуальними та корисними в контексті нелінійної динаміки і можуть допомогти у розумінні процесів на межі фаз.

Контроль бистабильности, осцилляций и хаоса в модельном электрокаталитическом процессе на поверхности сферического электрода

О.И. Гичан

Институт химии поверхности им. А.А. Чуйко Национальной академии наук Украины
ул. Генерала Наумова 17, Киев 03164, Украина, gichan@isc.gov.ua

Определена роль предшествующей химической реакции в возникновении трех динамических неустойчивостей, которые ведут к мультистабильности стационарных состояний, периодическим осцилляциям тока и возможному хаотическому поведению в модельном электрокаталитическом процессе на поверхности сферического электрода при потенциостатических условиях. Представлен краткий обзор класса неравновесных систем, где возникают такие неустойчивости, и рассмотрено их возможное применение по последним литературным данным. Полученные результаты являются актуальными и полезными в контексте нелинейной динамики и могут помочь в понимании процессов на межфазной границе.